CARBON 47 (2009) 829–838

available at www.sciencedirect.com

ScienceDirect

journal homepage: www.elsevier.com/locate/carbon

Tailoring multi-wall carbon nanotubes for smaller nanostructures

Jigang Zhou[a], *Joshua Cheiftz*[b], *Ruying Li*[b], *Fengping Wang*[a], *Xingtai Zhou*[a], *Tsun-Kong Sham*[a,*], *Xueliang Sun*[b,*], *Zhifeng Ding*[a,*]

[a]*Department of Chemistry, The University of Western Ontario, London ON, Canada N6A 5B7*
[b]*Department of Mechanical and Materials Engineering, The University of Western Ontario, London ON, Canada N6A 5B7*

ARTICLE INFO

Article history:
Received 17 July 2008
Accepted 18 November 2008
Available online 27 November 2008

ABSTRACT

Efficient electrochemical treatments of multi-wall carbon nanotubes (MWCNTs) in acetonitrile were performed by cycling the applied potential on a carbon paper grown with MWCNTs between −2.000 V and 2.000 V (vs $Ag/AgClO_4$) at a scan rate of 0.5 V/s. The tailored MWCNTs with obvious morphological modification could be further cut into short tubular structures through ultrasonic processing in ethanol. Various analytical techniques, including scanning electron microscopy, transmission electron microscopy, and X-ray photoelectron spectroscopy, were used to probe the morphological and structural evolution of MWCNTs during the treatments. The length of the shortened tubular structures ranged from a hundred to a few hundred nanometers, depending on the electrochemical procedures applied. The deformed and shortened MWCNTs displayed a graphitic crystalline structure. These results suggest that repeated electrochemical oxidation and reduction processing of MWCNTs opens up a new route to controlling surface modification and cutting of MWCNTs, which will facilitate their application in areas such as energy storage, catalytic support, and biosensing.

1. Introduction

Carbon nanotubes (CNTs) have found diverse applications in nanoscience and nanotechnology due to their unique chemical, mechanical, and electronic properties [1]. Recently, we reported that luminescent carbon nanocrystals could be prepared electrochemically from multi-wall carbon nanotubes (MWCNTs) [2]. The carbon nanocrystals are more attractive than their semiconductor counterparts due to their potential applications in optoelectronic devices and their lower toxicity [2,3]. While long CNTs/carbon nanotubules (μm) have significant applications in composite materials, short tubes or small carbon nanostructures, with controllable lengths and large active and accessible areas, should be advantageous for a broader range of applications. These include drug delivery, field emission, nanoelectronics, catalyst support, and energy storage or conversion. For instance, ensembles of long aligned carbon tubules [4] after deposition of catalyst nanoparticles, were found to be a good candidate for electrochemical energy storage and production. It is perceived that carbon nanostructures smaller than those tubules should be a better catalyst support due to their larger surface areas, making them accessible to catalyst deposition and thus catalytic reactions. But the increase in capacitive current should be carefully considered for the applications. Furthermore, tailoring the length of CNTs, especially down to the nanometer range, represents an effective and attractive means for electronic structure engineering, which might approach the limit of well-understood fullerene molecular clusters. However, due to the strong covalent sp^2-hybridized carbon bonds, the manipulation of CNTs presents

* *Corresponding authors:* Fax: +1 519 661 3022 (Z. Ding).
E-mail addresses: sham@uwo.ca (T.-K. Sham), xsun@eng.uwo.ca (X. Sun), zfding@uwo.ca (Z. Ding).
0008-6223/$ - see front matter © 2008 Elsevier Ltd. All rights reserved.
doi:10.1016/j.carbon.2008.11.032

numerous technical challenges [5]. Theses challenges include purification, solubility enhancement, and surface functionalization [6].

The cutting of long CNTs into shorter segments increases their surface area and offers a route to surface functionalization. Physical and chemical approaches for cutting CNTs exist and may be combined under specific conditions. The physical techniques include abrasion, grinding, ball milling, electrical cutting (positioning target tube followed by applying an electric field with the scanning tunneling microscopy tip), gamma irradiation, segmenting via lithography and sonication [7–13]. Chemical methods rely mainly on oxidation treatments including high temperature acid fluxing [14], ceric sulfate destructing [15], and fluorination followed by pyrolysis up to 1000 °C [16]. Although these techniques exhibit promise in CNTs processing, they are inefficient, produce low yields, and involve difficult purification steps. Electrochemical methods have been applied to etch individual CNTs [17] as well as open them up for hydrogen storage [18]. However, an effective production of deformed and cut CNTs has not yet been reported.

In this paper, we report the development of a facile and efficient electrochemical method for MWCNT processing in acetonitrile, followed by ultrasonic cutting in ethanol. Such a method provides tailored CNTs and minimizes undesirable by-products. The detailed morphological and structural features of these electrochemically tailored CNTs are herein presented and the mechanisms for their formation are also discussed.

2. Experimental section

2.1. MWCNT growth on carbon paper by chemical vapor deposition (CVD)

The synthesis of MWCNTs was carried out by decomposing ethylene on Co–Ni nanoparticles deposited on the fibers of a carbon paper in a specially designed CVD reactor [19]. The carbon paper consists of graphite carbon fibers and resin (E-TEK, Division of DeNora with 81% porosity). The catalyst preparation of Co–Ni nanoparticles is herein briefly described. The initial step involves the hydrolysis of 2-(4-chlorosulfonylphenyl) ethyl trichlorosilane (United Chemical Technologies, Bristol, PA) and subsequent proton exchange with Co and Ni ions. This produces a sulfonate solution of combined transition metal ions into which a piece of carbon paper was immersed for 10 s. Once dry, the carbon paper was heated at 500 °C for 10 min in a hydrogen atmosphere to reduce the absorbed Co and Ni ions. The resulting Co–Ni catalyst nanoparticles facilitate the growth of MWCNTs by decomposing ethylene at 850 °C. Such MWCNTs are henceforth denoted original CNTs. MWCNTs grown on carbon paper substrate display good electrical contact between the CNTs and carbon paper substrate [20].

2.2. Electrochemical and sonication treatments of MWCNTs

The CNT-covered carbon paper (original) was cut to fit in a Teflon jacket designed for making an electrical contact and exposing a disk-shaped surface with a geometrical area of 0.28 cm^2. The electrochemical cell consisted of this working electrode, a Pt coil counter electrode, and a $Ag/AgClO_4$ reference electrode in purified acetonitrile solution with 0.1 M of tetrabutylammonium perchlorate (TBAP) as the supporting electrolyte. The electrode potential could be calibrated by the known potential of ferrocenium/ferrocene (Fc/Fc^+) as 0.342 V vs a standard calomel electrode (SCE) in the same system [21]. The electrochemical treatment was performed by cycling with an applied potential between −2.000 V and 2.000 V (vs $Ag/AgClO_4$) at a scan rate of 0.5 V/s, using an electrochemical analyzer (CHI 601A, CH Instruments, Austin, TX). The treatment duration is described as cycling numbers. To investigate the electrochemical characteristics during the treatment process, cyclic voltammograms (CVs) with slow scan rate of 0.01 V/s were carried out on the CNT-covered carbon paper before and after the treatment as well as on a bare carbon paper as the background. The surface characteristics of these CNTs were also examined by electrochemical reduction of 10 mM ferricyanide.

After the above-described treatment, the modified CNT-covered carbon paper was removed from the solution and washed sequentially using pure acetonitrile, methanol and double distilled, deionized water. The paper was dried prior to analyses.

The above CNT-coated paper was then placed in a glass vial with ethanol and sonicated at 40 kHz for 30 min in a Bransonic ultrasonic bath (Branson Ultrasonics Corporation, USA) maintained at room temperature.

The CVs on the original CNT electrode and treated CNT electrode were performed in a 10 mM solution of $K_4Fe(CN)_6$ with 0.1 M of K_2SO_4 as the supporting electrolyte, with a Pt coil as the counter electrode and a saturated Ag/AgCl electrode as the reference.

2.3. Morphological and structural characterization of the CNTs

The morphological evolution of the tailored CNTs is initially examined by scanning electron microscopy (SEM) with a LEO 1540XB FIB/SEM, operated at 1 to 3 KV with a working distance (WD) of 4–6 mm. Size and structural changes of CNTs at various stages of the electrochemical processing were studied by a Philip CM10 transmission electron microscopy (TEM) at 80 KV on a JEOL 2010F High-resolution TEM (HRTEM) operated at 200 KV. The specimen preparations for TEM are as follows. After sonication, the diluted black dispersion was dropped on a 400 mesh carbon-coated copper grid and the solvent was evaporated in ambient atmosphere.

Further, structural and compositional analysis of the tailored CNTs after 1000 cycles (dispersion in ethanol after sonication) was carried out by X-ray photoelectron spectroscopy (XPS, Kratos Analytical, UK) with a monochromatic Al K(alpha) X-ray source operating at 14 kV and 15 mA (210 W). The dispersion was deposited onto Au foil and dried under ambient conditions. These conductive specimen were analyzed. The base pressure in the analysis chamber was less than 10^{-9} Torr. For survey and high resolution spectra, pass energies and energy steps of 160 eV and 0.7 eV, and 20 eV and 0.1 eV, were used, respectively. The XPS data was curve-fitted

using Casa XPS software version 2.2.107 with a background subtraction and Gaussian–Lorentzian line shapes. The energy scale was calibrated using a sputter-cleaned gold sample kept on the sample stage. The sharp and intense $4f_{7/2}$ peak of gold at 84.0 eV was used as a calibration standard. The main asymmetric peak was found at 284.5 ± 0.2 eV after the peak deconvolution of the C_{1s} spectrum of MWCNTs [22]. The peak was assigned to sp^2-hybridized graphite-like carbon atoms and carbon atoms bound to hydrogen atoms. All other peaks were assigned according to the literature [23].

3. Results and discussion

3.1. Electrochemical treatments

The application of electrochemistry as a processing treatment for CNTs requires that CNTs be in good electrical contact with the electrode. In the present study, CNTs were grown directly on a carbon paper substrates [24], which were suitable for the treatment. The conductive path between the CNTs and the carbon paper substrate is clearly shown by the current response in Fig. 1. Compared to bare carbon paper (Fig. 1b), the CNT-coated paper displays a much larger charging current which should be due in part to the large active surface area of the CNTs (Fig. 1a) [20]. The original CNTs have a unique scrolled structure consisting of a single graphene sheet rolled up to reveal many edge planes [24]. Compton et al. [25] demonstrated that the electrochemical reactivity of concentric CNTs resides solely at edge-plane-like sites and defects which occur at the end of the nanotubes, or along the tube axis. Our scrolled CNTs expose larger edge planes than the concentric CNTs. Thus higher charging current is expected.

The CV of the CNTs (solid) after 100 cycles scanning between −2.000 and 2.000 V in Fig. 1 shows a slightly larger charging current than that of the original CNTs (dashed). Note that the charging current will increase further with the increasing number of cycles [2]. This can be attributed to the increase in effective electrochemical area on the CNTs mainly through the electrochemical reactions and possible intercalation of the electrolyte ions. We will get back to this point later in this section on the assignment of redox peaks.

CVs of the CNTs in Fig. 1a shows that oxidations occur at about 0.6 and 1.5 V (their corresponding cathodic peaks are at 0.3 and 0.8 V), while reductions occur at about −1.1 V and −1.6 V (their correlating anodic peaks are at −0.7 and −1.4 V). Though the peaks are not well defined due to the higher capacitive current, they can be assigned to redox reactions involving defects and sidewalls based on previous studies of CNT, [2,25] SWNT [26] and porous carbon materials [27]. No significant changes were observed upon solution degassing with argon for 10 min, which caused only a small decrease in the cathodic current at negative potentials. Electrochemical reactions of CNTs at a glassy carbon electrode in aqueous solution have been reported although the redox peaks were not specifically assigned [28]. However, the peaks at potentials more positive than 0.200 V can be assigned to the oxidations of oxygen functional groups at the surface. The oxygen functional groups in such scrolled CNTs have been identified experimentally [29]. A similar electrochemical reaction, i.e. the protonation/deprotonation reaction of oxygen functionalities 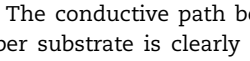 on SWCNT coated Teflon sheet [26] and CNT-coated Bucky paper [30] in aqueous solution has been reported. Similar to surface functionalities of porous carbon materials [27], these reactions are associated with surface oxygen complexes, i.e. the carbonyl/alcohol groups, and increased defect densities in CNTs which increase the hydrophilicity of the CNTs. Electrochemical reactions at potentials more negative than –1.1 V can be assigned to the reduction of oxygen functional groups on the CNT surfaces or molecular oxygen trapped within [26].

It is also observed that the double layer charging effect seen as the constant current background blurs the faradaic features especially under fast scanning. Therefore, detailed CV investigations for both bare carbon paper, and CNT-covered carbon paper, have to be performed under a slow scanning rate. CV in Fig. 1b shows that no significant faradaic reactions occurs (except the reduction of trapped oxygen at about −1 V) in the potential range of −1.8 V to 1.8 V for carbon paper. This result not only verifies the activity in CNTs relative to the carbon fibers but also allows for the assignment of the redox peaks of CNT-covered carbon paper to the CNT surface reactions. The CV of CNTs also demonstrates another

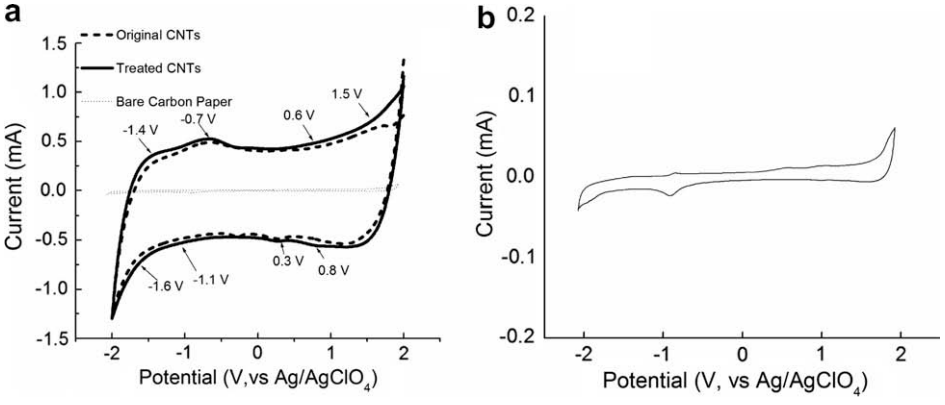

Fig. 1 – Cyclic voltammograms (CVs) of a bare carbon paper (dotted), original CNTs (dashed) and treated CNTs (solid, after 100 cycles scanning) in acetonitrile with 0.1 M of TBAP as the supporting electrolyte (a). Scanning rate is 0.01 V/s. CV of the bare carbon paper is magnified in (b) for comparison.

oxidation procedure when the potential is more positive than 1.5 V in the potential window. The observed oxidation potentials (0.6 and 1.5 V) closely match the reported electrochemical oxidation of carbon in aqueous solution. Thus they can be assigned to the reaction involving amorphous carbon on defect area (0.450 V vs Hg/HgO) and side wall (1.700 V vs Ag/AgCl) to form oxygen function groups, respectively [17,31].

More interestingly, the CV of CNTs after 100 cycles, Fig. 1a, is different from the CV of original CNTs. First of all, the charging current is slightly larger than that in the original CNTs as mentioned above, which we attribute to the enlargement of effective electrochemical area. It is different from the current decrease observed in CNTs electrochemically etched in aqueous electrolyte where severe oxidation totally etches away the CNTs [17]. A second feature in Fig. 1a is the manifestation of a redox pair at 0.8 and 1.5 V which suggests the increase of defect in CNTs. It is clear that the electrochemical treatment process is very complex in this present system and the details await further investigation. It should be emphasized that the effect of electrochemical treatment can also be easily observed by the color change in solution: from colorless to yellow and even to dark brown during the treatment. The solution emits blue luminescence upon irradiation with an UV lamp. The luminescent, water soluble product was purified by evaporating the acetonitrile from the solution, dissolving the remaining solid in water, and then dialyzing the aqueous solution with a cellulose ester membrane bag. This dialysis step removed most of the supporting electrolyte, TBAP, from the solution. Surprisingly, carbon nanocrystals (NCs) were observed by high-resolution electron transmission microscopy, which we recently reported elsewhere [2]. The generation of NCs also agrees well with the above electrochemical study, i.e. an increase of CNT surface area and defects. We have previously proposed that the intercalation of TBA^+ cations into scrolled CNTs caused the partial deformation and breaking of CNTs into the NCs [2]. Further detailed morphological and structural evolution is presented in the section of SEM and TEM characterization.

Upon closely looking at the electrochemical behavior in the CVs and the change in electrolyte solution color, it is plausible that TBA^+ intercalation caused more structural transformation than sole electrochemical oxidation did in the presence of oxygen; though oxidation might be the very first step to open up more accessible spots for the following intercalation. In fact, the cycling of the applied potential between 2.000 and −2.000 V leads to alternative oxidation and reduction reactions. Oxygen function groups are not expected to increase greatly. In contrast, the possible intercalation process is not fully reversible which causes the structural deformation/breaking of CNTs. It is worth mentioning that the scanning in the positive potential range only or in the negative potential range only did not change the solution color. This observation supports the above mechanisms in the electrochemical processing.

3.2. *Electrochemical reduction of ferricyanide on treated CNT-covered carbon papers*

The CV in 10 mM of $K_4Fe(CN)_6$ solution with 0.1 M of K_2SO_4 as the supporting electrolyte on tailored CNTs, Fig. 2, has a larger

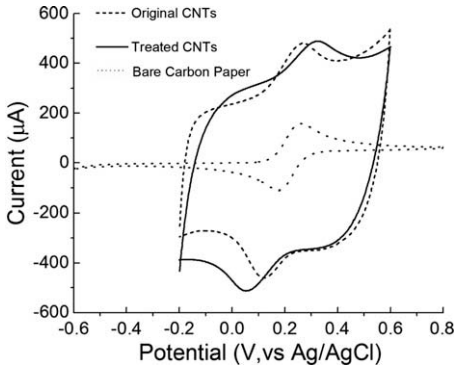

Fig. 2 – CVs of a bare carbon paper (dotted), original CNTs (dashed) and treated CNTs (solid) in 10 mM of $K_4Fe(CN)_6$ solution with 0.1 M of K_2SO_4 as the supporting electrolyte.

charging current than that on untailored CNTs, indicative of a larger surface area. This is consistent with the results shown in Fig. 1. More interestingly, the difference between cathodic and anodic peaks on treated CNTs is larger than that on the original CNTs, demonstrating less reversibility for the former. The increased defect density might cause an increase in resistance of the substrate, and therefore an augenmented electrochemical cell resistance, R. Furthermore, larger electrode surface after the electrochemical treatment showed a larger current, i. The two factors lead to an increased ohmic potential or iR drop, and therefore less reversibility for the oxidation of ferrocyanide. A larger separation between the anodic and cathodic peaks of the oxidation on the treated CNTs was therefore observed. This observation implies that the changes in structure in the rolled edges are caused by the electrochemical treatment. Moreover the CV pattern in CNTs agrees well with Compton et al. on the electrochemical behavior of the edge-plane-like sites in concentric CNTs [25].

3.3. *SEM and TEM Characterization of tailored CNTs*

In order to monitor the electrochemical treatments, systematic morphological and structural investigations by SEM and TEM were conducted on original CNTs and tailored CNTs at different stages of the treatment, as shown in Fig. 3 (a–c). It can be clearly seen from SEM images (images a1 and a2) that straight, high-density original CNTs typically have a diameter of 30–50 nm and length of 20 μm. This provides a large electrochemical reaction area as demonstrated in Fig. 1. Further observation by HRTEM, Fig. 3 (image a3), reveals that the original tube is composed of well organized carbon layers with a normal spacing of 0.34 nm. A closer inspection of the tube wall shows that the external and internal fringes terminate periodically at intervals of ~4 nm, as indicated by arrows. The presence of the fringe terminations suggests that the cylindrical tube has a scrolled structure. In this case, the cylindrical tube is generated by scrolling a single graphene sheet. A more detailed description of structural characteristics of the scrolled tube can be obtained from previous work [24]. It is worth mentioning that this kind of scrolled tube structure will facilitate the deformation and breaking of the tube during electrochemical treatments. Indeed, it has been

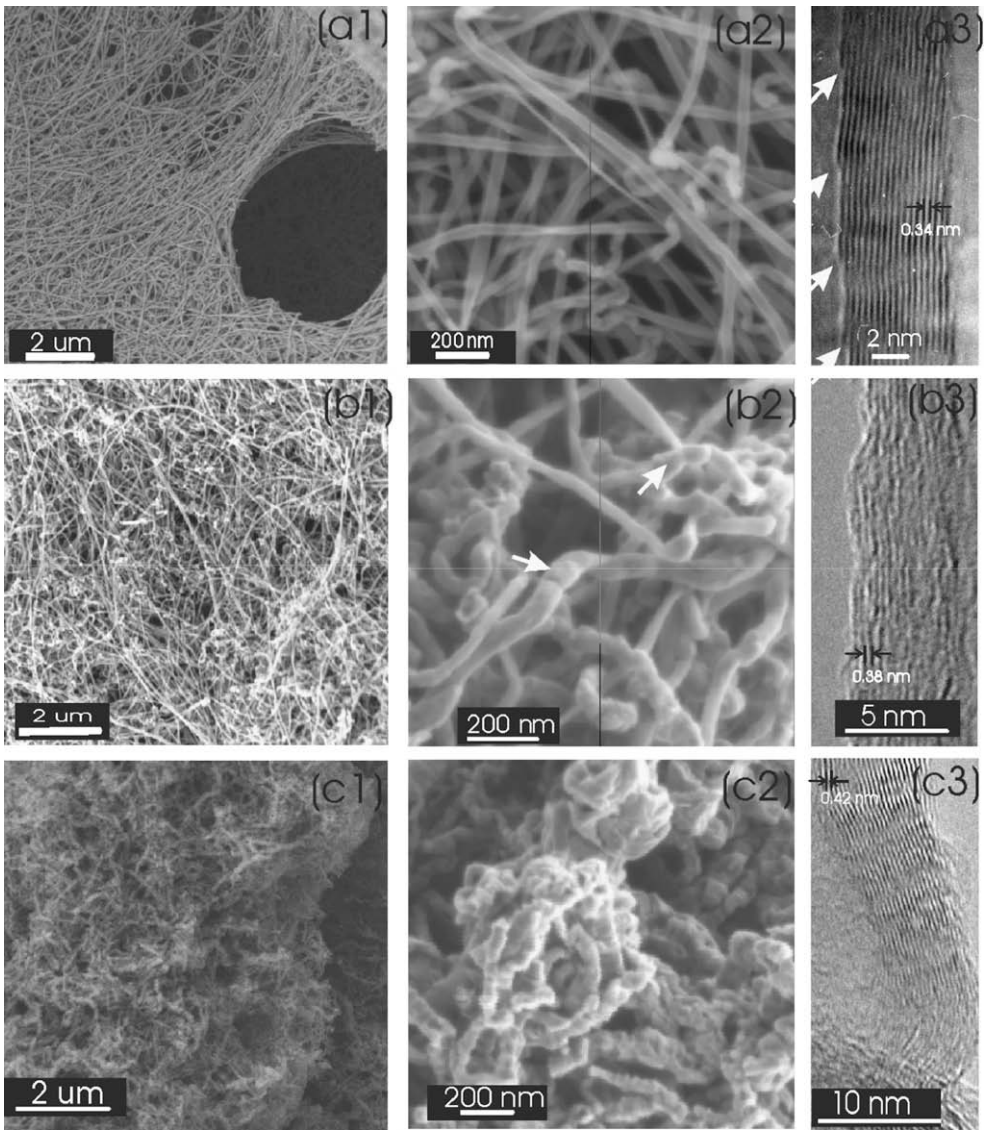

Fig. 3 – CNT morphology evolution during the electrochemistry treatments. SEM (a1–a2) and HETEM (a3) images of original CNTs. SEM (b1–b2) and HRTEM (b3) images of CNTs after 100 cycles scanning. SEM (c1–c2) and HRTEM (c3) images of CNTs after 1000 cycles scanning. The lattice space was labeled in HRTEM. The arrows in (a3) indicate the external and internal fringes on CNTs.

reported that the electrochemical response from carbon strongly depends on the physicochemical properties including purity and crystalline structure [31]. Here, the fringes in the scrolled structure of CNTs can provide easily accessible chemical or electrochemical paths which will benefit the surface deformation during electrochemical treatments.

After 100 cycles, no evident length change of the CNTs is observed (images b1 to b3 in Fig. 3). However, the morphology of CNTs reveals significant modification, as displayed by image b2 in Fig. 3. In this case, compared with straight tubes in image a2, most of the tailored CNTs show bent and curled features and a rugged surface. Further scrutiny of the tailored CNTs by HRTEM revealed more detail in the structural change (image b3 in Fig. 2). Some areas displayed lattice interruptions. Furthermore, the average lattice spacing after examination of a few tubes is 0.38 nm, which is greater than the normal tubes by 0.04 nm. The lattice spacing increase could correspond to species intercalated into CNTs. A TBA^+ cation should occupy a volume of 0.2 nm. Since TEM was carried out after electrochemical treatment, the deformation due to TBA^+ intercalation might not be readily evident. For instance de-intercalation might happen during the washing process with acetonitrile, methanol and water when air is exposed to the treated CNTs. The relatively small increase in lattice spacing could be due to the chemical modification of the graphene plane, the presence of defects or the residual deformation after the breaking of CNTs. Currently, it is not very clear which factors result in the lattice increase. However, it is almost certainly that the transport of the TBA^+ cations in and out of the graphene layers during the electrochemical process plays a very important role. This point will be reexamined in the following XPS section. Amorphous carbon

was also generated during this period as revealed by the blurred TEM image. The extent of disorder increases in time as can be seen in the HRTEM of CNTs after 1000 cycles.

Electrochemical treatments after 1000 cycles resulted in a larger deformation of all CNTs. No straight-line morphological feature of nanotubes is observed and the tubes look much shorter, as shown in Fig. 3(c1). The SEM image of these tubes, Fig. 3(c2), reveals rougher surfaces and seriously damaged tubes. In addition, a larger disordered structure of these tailored CNTs can be seen with HRTEM, Fig. 3(c3). The lattice spacing of some areas has increased to a value of up to 0.42 nm. Besides the larger spacing distance there are more lattice interruptions which slid relatively and form islands. The islands are absent in Fig. 3(a3). Such islands are expected to be finally released as freestanding carbon NCs to solution.

3.4. *Sonication after the electrochemical treatment*

The final step of the cutting of CNTs was carried out by sonication at room temperature in ethanol for 30 min after 100 scanning cycles. After the sonication, most of the tubes detached from the carbon fibers of the carbon paper substrate. A typical TEM image is shown in Fig. 4. Several interesting features can be observed. First, the tailored tubes, originally 15 μm in length, are broken down into segments which range in size ranging from a few microns to 100 nm, as indicated by (a) and (b) in Fig. 4. Second, a rough surface can be clearly observed, marked by a circle (D) and the inset, which corresponds to SEM observations in Figs. 3(b2) and (b3). Third, an open area indicated by (e) is visible, suggesting that further cutting will occur from this area. Finally, the metal catalytic nanoparticles encapsulated by the graphitic layers are still visible (Fig. 4). The presence of metallic nanoparticles, after electrochemical treatments, suggests an interesting mechanism different from that in conventional acid etching. Usually, the oxidation occurs in areas of graphene covered metal catalytic nanoparticles when the tubes are immersed in acidic solution. In that case, the metal nanoparticles are removed, as previously observed [19]. However, many metal particles still exist and are covered by graphitic layers in this present study, indicating that there may be other factors which dominate the deformation and the cutting process. This observation supports the TBA^+ intercalation mechanism, which is favored on edge-plane-like sites but not on sealed sites with capped catalysts. In addition, an investigation of the opened tip of one tube by HRTEM, Fig. 4b, reveals a mixture of graphitic layers and disordered structure. The gra-

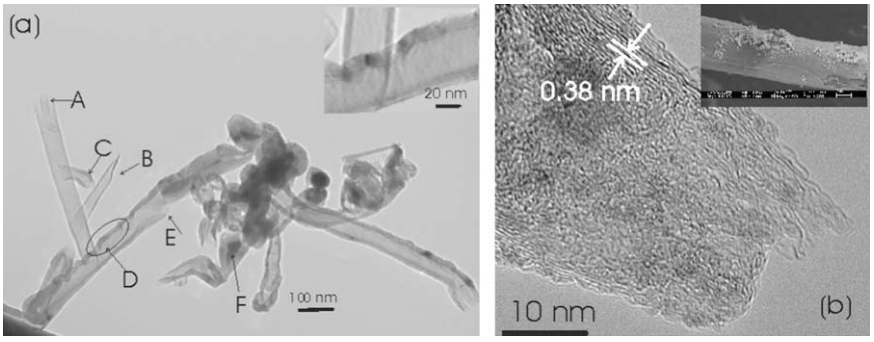

Fig. 4 – TEM images of short CNTs obtained from CNTs after ultrasonication treatment following 100 cycles of potential scanning. (a) Regular TEM. The inset in (a) is the close up of region D in this image. (b) HRTEM of one end of a shorten CNT. The inset in (b) illustrates a bare carbon fiber after electrochemistry and sonication treatment, where the scale bar is 2 μm.

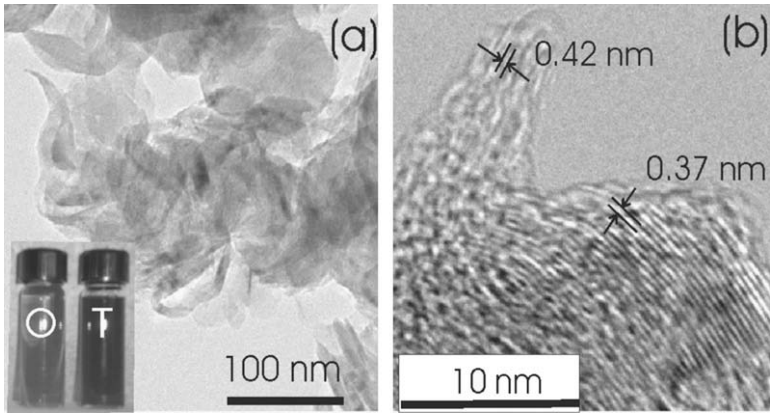

Fig. 5 – TEM images of short flake-like carbon structure obtained from CNTs after ultrasonication treatment following 1000 cycles of potential scanning. (a) Regular TEM. (b) HRTEM. The inset in (a) shows the dispersion of original (O) and tailored (T) CNTs in ethanol after ultrasonication treatment.

phitic layers have a spacing distance of 0.38 nm, which agrees well with Fig. 3(b3).

The cutting of CNTs by sonication after 1000 cycles led to more interesting features. SEM and TEM investigations demonstrated that no more CNTs exist on the carbon fibers (not shown here) after the sonication. However, the ethanol solution changed color from colorless to dark brown, as shown in the inset of Fig. 5. Further, the solution with dark brown color did not show any solid settle down and kept a clear dark color after long-standing, which suggested increasing hydrophilicity of obtained carbon structures. By careful examination of the solution deposits by HRTEM, two kinds of carbon nanostructures can be observed. One consists of a chain of pieces with a diameter of ~30 nm and length of ~100 nm (Fig. 5a). A closer observation by HRTEM clearly shows that each piece still has the same graphitic structure as the nanotubes (Fig. 5b). The other structure is NCs, which were generated by the electrochemical treatment [2]. After placing a droplet of the solution on a TEM grid, a high-density of NCs can be seen (Fig. 6). The typical NCs have a diameter of ~3 nm with graphitic structure and a 0.34 nm lattice spacing (inset in Fig. 6). Further studies found that such NCs have highly efficient luminescent effects which have recently been reported in detail elsewhere [2]. It is also anticipated that these NCs will have various applications in biology labeling and optoelectronic devices.

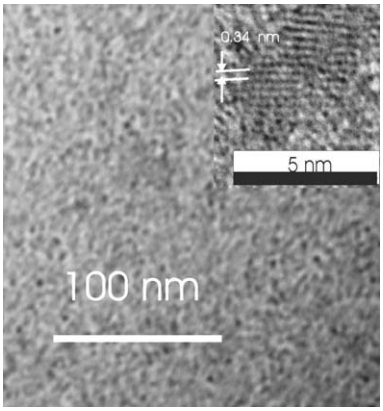

Fig. 6 – TEM of luminescent carbon nanocrystals in electrolyte solution during the electrochemically treating of CNTs.

3.5. *XPS analysis of tailored CNTs*

To understand the cutting procedure of CNTs and characterize the composition of the tailored CNTs, XPS is used to analyze the CNTs after 1000 cycles. XPS spectra are shown in Fig. 7. The survey spectrum shows the existence of C (90.1%), O (8.3%) and N (1.6%) in the sample. A fitted C 1s core level photoelectron spectrum reveals peaks at 284.5, 285.1, 286.3, and 291.0 eV which could be assigned to sp^2 in graphite, defect-containing sp^2 in amorphous carbon or alcohols, sp^3 defects, and π to π^* shake up associated with the graphitic carbon, respectively [15]. It is evident that the majority of C 1s photoelectrons from carbon atoms originated from sp^2 bonding which is expected and agrees well with the conclusion

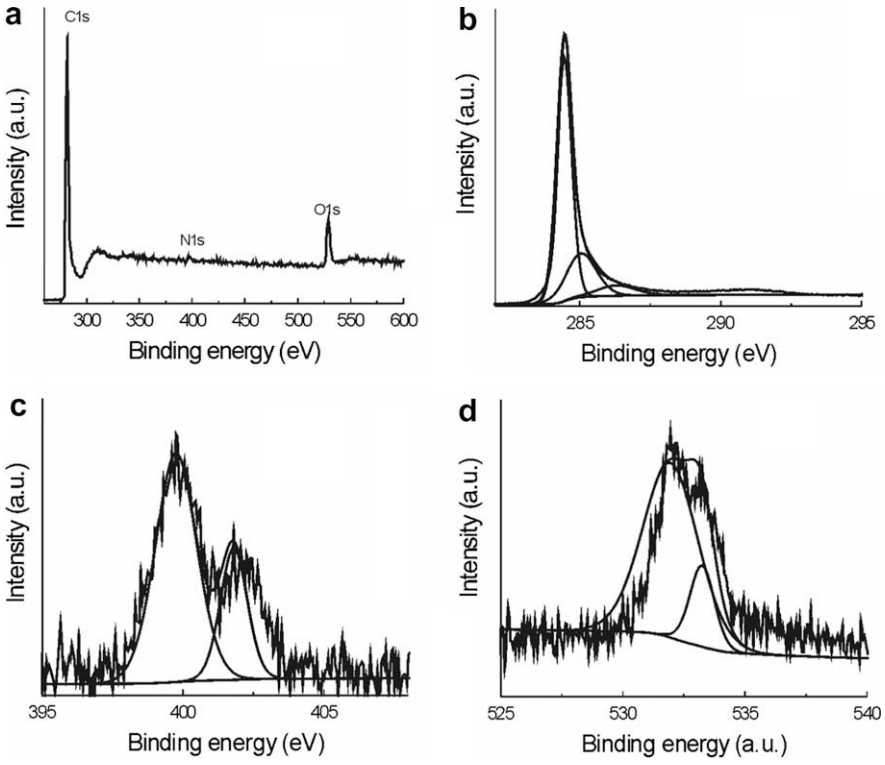

Fig. 7 – XPS of CNTs after 1000 cycles of potential scanning. (a) Survey spectrum. (b) High resolution spectrum of C1s. (c) High resolution spectrum of N1s. (d) High resolution spectrum of O1s.

obtained from Figs. 1 and 2. The full width at half maximum (FWHM) of sp^2 carbon component, 0.67 eV, also agrees with the conclusion that only mild defect generation occurs after such treatment as compared with other harsh treatment processes where significant linewidth broadening due to chemical inhomogeneity will result [15]. The existence of defect-containing sp^2 carbon atoms is associated with surface structure disorder as revealed by SEM and TEM. An O 1s core level photoelectron spectrum with binding energy centered on 531.95 and 533.25 eV can be attributed to the possible existence of carbonyl or alcohol functional groups [10] as well as carboxylic acid [23]. These oxygen functional groups are consistent with air oxidation of the surface and opened ends due to exposure to air during electrochemical treatment. The existence of such hydrophilic groups in tailored CNTs can also be related to the observation of good dispersion in alcohol as shown in Fig. 5a inset. Most interestingly, the presence of N in the tailored CNTs, with binding energies of 399.75 and 401.8 eV, is observed after electrochemical treatments in acetonitrile solution. The intensive washing and drying can prevent physical absorbing of acetonitrile on CNTs. Therefore, the presence of nitrogen could be attributed to the intercalation of N containing species into CNTs during electrochemical treatment. The binding energy values allow us to assign the peaks to acetonitrile [23] and/or pyridine-like N and graphite-like N [32] in CNTs. We are not able to identify the species corresponding to the binding energy of 401.8 eV. We believe that the possible intercalation of TBA^+ involves an interaction between N (in TBA^+) and C in (CNTs). The discrepancy between the fit and the data simply reflect the presence of several chemically different N and O sites on the surface.

XPS of the carbon paper substrate, original CNTs and CNTs after 100 cycles of potential scanning were not carried out. As reported by Ago et al. [22], the ratio of the carbon in the oxygen function groups to all the carbon atoms detected did not vary more than 10% from purified CNTs to CNTs which underwent oxidation in the extreme conditions (such as at high temperature, in contact with highly oxidative acids). As analyzed in Section 3.1, the electrochemical treatment was in very mild conditions and the CNTs underwent oxidation followed by reduction in the cycling of the applied potential. The above ratio is expected to change in much less than 10% after various cycles of potential scanning.

3.6. *Summary*

We have reported that CNTs can be fragmented into significantly shortened and deformed CNTs and ultimately CNCs by electrochemical treatment in acetonitrile solution, followed by sonication in ethanol. Based on the morphological and structural observations by SEM and TEM as well as compositional analysis by XPS, we propose a mechanism for the deformation and the cutting of the tubes as illustrated schematically in Fig. 8 and discussed below.

(i) After 100 cycles of the electrochemical treatments in acetonitrile solution containing 0.1 M TBAP, the straight tubes become bent and reveal very roughened surfaces, as indicated by Fig. 8(a and b). At the same time, nanocrystals (NCs) are released from CNTs into the electrolyte solution. Further sonication in ethanol generates short tubes with sizes

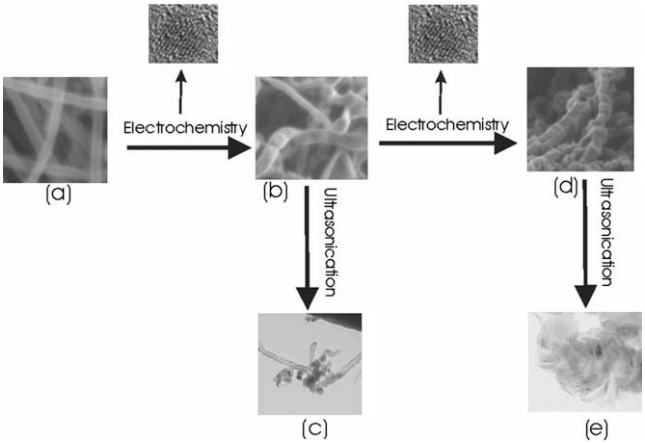

Fig. 8 – Illustration of the processes to generate luminescent carbon nanocrystals and shortened CNTs by the electrochemistry and the ultrasonication.

ranging from a hundred to a few hundred nanometers (Fig. 8c). It is believed that the interruption points observed in Fig. 3(b3) are the broken points.

The intercalation process in carbon is well-understood and has been applied in graphite intercalation compounds (GICs) in which ions or molecules can be inserted into graphite interlayers to form intercalation [33]. Recently, a similar process has been reported for CNTs. Hydrogen insertion into CNTs clearly shows a disturbed host lattice from the original ordered structure [34]. In our study, XPS confirms that there are N containing species present in the tailored CNTs. More recently, further evidence has been provided for acetonitrile intercalation into CNTs; especially the structure of CNTs, named by "edge-plane-like defect sites", plays a significant role in the intercalation [23]. As mentioned above, the tubes used in our work have scrolled structures which are similar to the "edge-plane-like defect sites". Therefore, the tube structure and the possible intercalation are associated with deformation, breaking and cutting of the tubes during electrochemical and ultrasonic treatments in our study. Two things are still open to discussion: first, what species is intercalated into the tube? From HRTEM we do not observe TBA^+ remaining in the tailored nanostructures. XPS results allow us to conclude that N containing species existed in tailored CNTs. We have not identified the species involved. However, we do observe that TBA^+ is still essential to the deformation process because it does not occur in acetonitrile solution with lithium percholorate. This allows us to propose that TBA^+ at least facilitates the acetonitrile intercalation in the form of co-intercalation molecules in CNTs.[23] This interaction might be TBA^+ solvated by acetonitrile. Second, as to the details of the local chemical environment of N in the tailored CNTs, research using X-ray absorption fine structure spectroscopy (XAFS) is underway.

(ii) Longer electrochemical treatment such as 1000 cycles introduces more N resulting in larger deformation and lattice spacing (from 0.34 nm to ~0.40 nm in this study). This produces a rougher tube surface (Fig. 8d) and some NCs in the solution. Further sonication in ethanol releases carbon chains ~30 nm in diameter and ~100 nm in length in the solution

(Fig. 8e) leading to high water solubility as observed in the inset of Fig. 5.

From the discussion above, our electrochemical treatment has advantages in the controllability via treatment duration and mild reaction conditions, leading to a CNT surface deformation and an increase in defects on edge-plane-like sites. The treatment paves the way for sonication cutting of the CNTs into small carbon nanostructures.

4. Conclusion

A simple method that combines electrochemical and sonication treatments has been developed to deform and cut MWCNTs. The deformed nanotubes displayed bent morphologies and a larger lattice spacing of up to 0.42 nm. The cut nanotubes vary in length from a few hundred nanometers to a few nanometers, which might be controlled by the number of cycles of potential scanning in the electrochemical treatments. The modification mechanisms are likely linked to the unusual scrolled nanotube structure and the electrolyte solution. The deformed and shortened nanotubes are envisaged to become important candidate materials for many potential applications in energy storage, catalytic support and biosensing.

Acknowledgement

We appreciate the financial support of the Natural Sciences and Engineering Research Council of Canada (NSERC, New Discovery and Equipment Grants), Ontario Photonics Consortium (OPC), Canada Foundation for Innovation (CFI), Ontario Innovation Trust (OIT), the Premier's Research Excellence Award (PREA) and the University of Western Ontario (Academic Development Fund (ADF) and the Start-up Fund). X. Sun and T.K. Sham acknowledge the support of the CRC (Canada Research Chair) program. The Ding, Sun and Sham groups are members of the Center for Chemical Physics (CCP) and the Western Institute of Nano Science (WINS) at UWO. ZFD is grateful to the Swiss Federal Institute of Technology in Lausanne (EPFL) for a visiting professorship in Prof. Hubert Girault's group during the summer 2003. Technical assistance from John Vanstone, Jon Aukima, Sherrie McPhee, Mary Lou Hart and Marty Scheiring is gratefully acknowledged. We are in debt to Todd Simpson, Fred Pearson, Ronald Smith, Mark Biesinger, Leo Lau, Brad Kobe, Bradley Payne, Rob Lipson, Ian Mitchaell, and David Shoesmith for their kind help and fruitful discussions.

REFERENCES

[1] Baughman RH, Zakhidov AA, de Heer WA. Carbon nanotubes-the route toward applications. Science 2002;297(5582):787–92.
[2] Zhou J, Booker C, Li R, Zhou X, Sham T-K, Sun X, et al. An electrochemical avenue to blue luminescent nanocrystals from multiwalled carbon nanotubes (MWCNTs). J Am Chem Soc 2007;129(4):744–5.
[3] Bard AJ, Ding Z, Myung N. Electrochemistry and electrogenerated chemiluminescence of semiconductor nanocrystals in solutions and in films. In: Peng X, editor. Structure and bonding. Berlin: Springer; 2005. p. 1–57.
[4] Che G, Lakshmi BB, Fisher ER, Martin CR. Carbon nanotubule membranes for electrochemical energy storage and production. Nature 1998;393(6683):346–9.
[5] Daraio C, Nesterenko VF, Aubuchon JF, Jin S. Dynamic nanofragmentation of carbon nanotubes. Nano Lett 2004;4(10):1915–8.
[6] Xing Y, Li L, Chusuei CC, Hull RV. Sonochemical oxidation of multiwalled carbon nanotubes. Langmuir 2005;21(9):4185–90.
[7] Pierard N, Fonseca A, Konya Z, Willems I, Van Tendeloo G, Nagy JB. Production of short carbon nanotubes with open tips by ball milling. Chem Phys Lett 2001;335(1–2):1–8.
[8] Stepanek I, Maurin G, Bernier P, Gavillet J, Loiseau A, Edwards R, et al. Nano-mechanical cutting and opening of single wall carbon nanotubes. Chem Phys Lett 2000;331(2–4):125–31.
[9] Peng J, Qu X, Wei G, Li J, Qiao J. The cutting of MWNTs using gamma radiation in the presence of dilute sulfuric acid. Carbon 2004;42(12–13):2741–4.
[10] Yang D-Q, Rochette J-F, Sacher E. Controlled chemical functionalization of multiwalled carbon nanotubes by kiloelectronvolt argon ion treatment and air exposure. Langmuir 2005;21(18):8539–45.
[11] Jeong S-H, Lee O-J, Lee K-H, Oh SH, Park C-G. Preparation of aligned carbon nanotubes with prescribed dimensions: template synthesis and sonication cutting approach. Chem Mater 2002;14(4):1859–62.
[12] Lustig SR, Boyes ED, French RH, Gierke TD, Harmer MA, Hietpas PB, et al. Lithographically cut single-walled carbon nanotubes: controlling length distribution and introducing end-group functionality. Nano Lett 2003;3(8):1007–12.
[13] Kukovecz A, Kanyo T, Konya Z, Kiricsi I. Long-time low-impact ball milling of multi-wall carbon nanotubes. Carbon 2005;43(5):994–1000.
[14] Liu J, Rinzler AG, Dai H, Hafner JH, Bradley RK, Boul PJ, et al. Fullerene pipes. Science 1998;280(5367):1253–6.
[15] Luong JHT, Hrapovic S, Liu Y, Yang D-Q, Sacher E, Wang D, et al. Oxidation, deformation, and destruction of carbon nanotubes in aqueous ceric sulfate. J Phys Chem B 2005;109(4):1400–7.
[16] Gu Z, Peng H, Hauge RH, Smalley RE, Margrave JL. Cutting single-wall carbon nanotubes through fluorination. Nano Lett 2002;2(9):1009–13.
[17] Ito T, Sun L, Crooks RM. Electrochemical etching of individual multiwall carbon nanotubes. Electrochem Solid-State Lett 2003;6(1):C4–7.
[18] Skowronski JM, Scharff P, Pfander N, Cui S. Room temperature electrochemical opening of carbon nanotubes followed by hydrogen storage. Adv Mater 2003;15(1):55–7.
[19] Sun X, Stansfield B, Dodelet JP, Desilets S. Growth of carbon nanotubes on carbon paper by Ohmically heating silane-dispersed catalytic sites. Chem Phys Lett 2002;363(5,6):415–21.
[20] Sun X, Li R, Villers D, Dodelet JP, Desilets S. Composite electrodes made of Pt nanoparticles deposited on carbon nanotubes grown on fuel cell backings. Chem Phys Lett 2003;379(1–2):99–104.
[21] Bae Y, Myung N, Bard AJ. Electrochemistry and electrogenerated chemiluminescence of CdTe nanoparticles. Nano Lett 2004;4(6):1153–61.
[22] Ago H, Kugler T, Cacialli F, Salaneck WR, Shaffer MSP, Windle AH, et al. Work functions and surface functional groups of multiwall carbon nanotubes. J Phys Chem B 1999;103(38):8116–21.
[23] Wildgoose GG, Hyde ME, Lawrence NS, Leventis HC, Jiang L, Jones TGJ, et al. 4-Nitrobenzylamine partially intercalated into graphite powder and multiwalled carbon nanotubes: characterization using X-ray photoelectron spectroscopy and

in situ atomic force microscopy. Langmuir 2005;21(10):4584–91.
[24] Sun X, Li R, Stansfield B, Dodelet J-P, Ménard G, Désilets S. Controlled synthesis of pointed carbon nanotubes. Carbon 2007;45(4):732–7.
[25] Banks CE, Crossley A, Salter C, Wilkins SJ, Compton RG. Carbon nanotubes contain metal impurities which are responsible for the "electrocatalysis" seen at some nanotube-modified electrodes. Angew Chem Int Ed 2006;45(16):2533–7.
[26] Barisci JN, Wallace GG, Baughman RH. Electrochemical studies of single-wall carbon nanotubes in aqueous solutions. J Electroanal Chem 2000;488(2):92–8.
[27] Bleda-Martínez MJ, Lozano-Castelló D, Morallón E, Cazorla-Amorós D, Linares-Solano A. Chemical and electrochemical characterization of porous carbon materials. Carbon 2006;44(13):2642–51.
[28] Li Y, Shi X, Hao J. Electrochemical behavior of glassy carbon electrodes modified by multi-walled carbon nanotube/surfactant films in a buffer solution and an ionic liquid. Carbon 2006;44(13):2664–70.
[29] Zhou J, Zhou X, Sun X, Li R, Murphy M, Ding Z, et al. Interaction between Pt nanoparticles and carbon nanotubes – An X-ray absorption near edge structures (XANES) study. Chem Phys Lett 2007;437(4–6):229–32.
[30] Kaempgen M, Roth S. Ultra microelectrodes from MWCNT Bundles. Synth Met 2005;152(1–3):353–6.
[31] Fang H-T, Liu C-G, Liu C, Li F, Liu M, Cheng H-M. Purification of single-wall carbon nanotubes by electrochemical oxidation. Chem Mater 2004;16(26):5744–50.
[32] Chen H, Yang Y, Hu Z, Huo K, Ma Y, Chen Y, et al. Synergism of C5N six-membered ring and vapor-liquid-solid growth of CN_x nanotubes with pyridine precursor. J Phys Chem B 2006;110(33):16422–7.
[33] Setton R. The graphite intercalation compounds: their uses in industry and chemistry. Synth Met 1988;23(1–4):467–473.
[34] Pekker S, Salvetat J-P, Jakab E, Bonard J-M, Forró L. Hydrogenation of carbon nanotubes and graphite in liquid ammonia. J Phys Chem B 2001;105(33):7938–43.